analytical chemistry

Article

pubs.acs.org/ac

FT-IR Spectroscopic Imaging of Reactions in Multiphase Flow in Microfluidic Channels

K. L. Andrew Chan and Sergei G. Kazarian*

Department of Chemical Engineering, Imperial College London, South Kensington Campus, SW7 2AZ, U.K.

Supporting Information

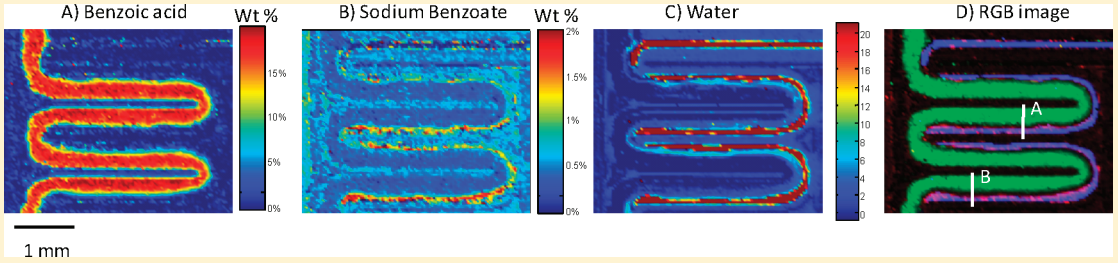

ABSTRACT: Rapid, in situ, and label-free chemical analysis in microfluidic devices is highly desirable. FT-IR spectroscopic imaging has previously been shown to be a powerful tool to visualize the distribution of different chemicals in flows in a microfluidic device at near video rate imaging speed without tracers or dyes. This paper demonstrates the possibility of using this imaging technology to capture the chemical information of all reactants and products at different points in time and space in a two-phase system. Differences in the rates of chemical reactions in laminar flow and segmented flow systems are also compared. Neutralization of benzoic acid in decanol with disodium phosphate in water has been used as the model reaction. Quantitative information, such as concentration profiles of reactant and products, can be extracted from the imaging data. The same feed flow rate was used in both the laminar flow and segmented flow systems. The laminar flow pattern was achieved using a plain wide T-junction, whereas the segmented flow was achieved by introducing a narrowed section and a nozzle at the T-junction. The results show that the reaction rate is limited by diffusion and is much slower with the laminar flow pattern, whereas the reaction is completed more quickly in the segmented flow due to better mixing.

Reactions in microfabricated devices have shown many advantages over traditional process systems.[1] The rapid development of microprocesses involving micromixers and microreactors requires more complex microdevices.[2−4] Although optimization of the process systems often uses numerical simulated models, validation of these models requires experimental measurements of concentration of present chemicals at various points in time and space within the system.[5] Therefore, the development of suitable characterization tools is important. To date, fluorescence imaging has been the method of choice for small-volume detection due to its exceptional sensitivity.[6] The use of a dye for visible detection is also proven to be a popular method due to ease of use. However, label-free detection methods remain an attractive alternative as there is no disturbance to the system studied. Furthermore, unlike methods that use labeling or dyes, label-free detection methods are not restricted to studies of reactions that produce a color change, such as acid−base reactions or reactions that yield colored species, because the detection principles are based on the structure of the chemicals. These methods such as NMR,[7] Raman,[8,9] including coherence anti-Stoke Raman[10] and surface-enhanced Raman,[11] and infrared spectroscopy[12] are some of the methods that have shown to be promising tools for chemical analysis in microfabricated devices.

Fourier transform infrared (FT-IR) spectroscopic imaging is a label-free imaging tool that can detect multiple components simultaneously. The chemical specificity of this technique arises from the intrinsic molecular vibrations which result in the measured spectrum. The low energy of infrared radiation also eliminates issues such as photodegradation or photobleaching. The focal plane array (FPA) detector, which consists of up to 16 384 pixels, enables the collection of thousands of spatially resolved infrared spectra for the generation of various chemical maps representing the spatial distribution of the particular components in the system. These maps are often referred as "chemical images" which can be used to study a wide range of samples, including microfluidic flows.[13] We have recently demonstrated that FT-IR imaging can be applied to image mixing of H_2O and D_2O with consecutive isotope exchange in laminar flow in a single-phase flow using a Y-junction microfluidic device[14] and to capture "chemical movies" in segmented flow using a T-junction microfluidic device.[15] The FPA detector has also been used, although not for imaging, to extract spatially resolved infrared spectra from a microreactor in a model catalyst system.[16] In this paper, we demonstrate that

Received: January 3, 2012
Accepted: April 2, 2012
Published: April 2, 2012

   dx.doi.org/10.1021/ac300019m | *Anal. Chem.* 2012, 84, 4052−4056

Scheme 1. Neutralization of Benzoic Acid with Disodium Phosphate at the Interface between Decanol and Water

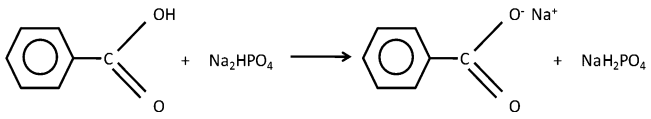

FT-IR imaging can be used to study chemical reactions in a two-phase system in both laminar and segmented flow microfluidics. Neutralization of benzoic acid dissolved in decanol with disodium phosphate (Na_2HPO_4) in water (see Scheme 1) has been used as the model reaction.

EXPERIMENTAL SECTION

Reagents. The 6.2 wt % Na_2HPO_4 (Sigma-Aldrich) solution is made by stirring weighted Na_2HPO_4 powder in deionized water until all solids are dissolved. The 15 wt % benzoic acid in decanol solution is made by stirring weighted benzoic acid powder in decanol (Sigma-Aldrich) until all solid are dissolved. All reagents are used as received.

FT-IR Spectroscopic Imaging. An infrared spectrometer (IFS66s, Bruker Optics, Germany) equipped with a macro-chamber attachment (IMAC, Bruker Optics) and a horizontal macrotransmission accessory was used to allow the microfluidic device to be imaged in a horizontal position. Further details about this accessory can be found elsewhere.[17] A 96 × 96 focal plane array detector (40 μm per pixel) was used to generate an imaging area of 3.84 mm × 3.84 mm with a lateral spatial resolution of 40 μm. The data were collected using OPUS 5.5 (Bruker Optics, Germany), which has a kinetic imaging mode for fast image capture of the segmented flow system.[15] Spectra were measured at 8 cm^{-1} for the laminar flow system and 16 cm^{-1} resolution for the segmented flow system. The number of coadded frames used in laminar flow measurements was 10, which gives a total scanning time of ~5 s. Single scan (kinetic mode) was used for the segmented flow experiment. With the 96 × 96 FPA and a spectral range of 1950−988 cm^{-1} the scanning time per image was ~93 ms.

Microfluidic Device Fabrication. There are many methods to create microfluidic devices.[18] The devices used here were fabricated in a similar manner as described by us previously.[19] In brief, a droplet-on-demand microdroplet printing system (AutoDrop, MicroDrop) consisting of a heated dispensing nozzle head and an *xyz* position robotic arm was used. Molten paraffin (mp 58−62 °C, Sigma-Aldrich) was directly printed by the system to create the microfluidic device on a CaF_2 infrared transparent window which is then sandwiched with another CaF_2 window to form sealed channels. Further details concerning the fabrication process can be found elsewhere.[19]

Laminar Flow Microfluidics. Laminar flows was generated by introducing the Na_2HPO_4 solution in water through a narrower channel from the right (380 μm wide, 25 μm height) and oil phase (decanol) via a wider channel from the top (450 μm wide, 25 μm height) where they join at a "T-junction". The joint stream then enters a serpentine region (450 μm wide, 25 μm height) with two 90° and three 180° turns before exiting the device.

Segmented Flow Microfluidics. Segmented flow was generated by introducing the Na_2HPO_4 solution through a nozzle (50 μm wide, 25 μm height) and a continuous oil phase (decanol) via a narrow channel (100 μm wide, 25 μm height). The joint stream then enters a wide serpentine region (480 μm wide, 25 μm height) with two 90° and three 180° turns before exiting the device. The speed and size of individual droplets can be controlled by the volumetric flow rates of both streams.

A liquid cell with CaF_2 windows (Omni Cell, Specac Ltd., U.K.) and 25 μm spacers was used as the substrate. The surface of CaF_2 windows was coated with a thin layer of polystyrene by casting 0.5 wt % polystyrene from toluene to provide hydrophobic surfaces inside channels. The film thickness was approximately 680 nm. In all cases, the device was connected to polyethylene tubing for injection of liquids into the device. Precision syringe pumps (PHD 2000, Harvard Apparatus) were used to deliver the fluids into the channel with the flow rate of 0.5 and 1 μL/min for benzoic acid in decanol and Na_2HPO_4 solution, respectively.

RESULTS AND DISCUSSION

The reaction chosen in this work is the formation of sodium benzoate from benzoic acid with Na_2HPO_4 following Scheme 1. Benzoic acid is only slightly soluble in water, whereas its sodium salt form is highly soluble (~200 times more soluble). Decanol was therefore used as the carrier of benzoic acids, whereas deionized water was used as the carrier for Na_2HPO_4. Decanol and water are not miscible, meaning the reaction between benzoic acid and Na_2HPO_4 can only happen at the interface. The two fluids are brought into contact in the microfluidic channel in a controlled manner where the product sodium benzoate dissolves in the aqueous phase.

Since the microfluidic channels were created by wax printing, decanol was used as the oil phase such that the paraffin wall would not disintegrate during the experiment. Na_2HPO_4 was used rather than NaOH to prevent the attack of NaOH on the paraffin wall. Other more chemically resistant materials for the channel walls may be investigated for use in the future such as "liquid Teflon" as introduced by Rolland et al.[20]

The flow rate of benzoic acid in decanol was 0.5 μL/min, while the Na_2HPO_4 solution flow rate was 1 μL/min. Two designs of microfluidic devices were created to generate the laminar and segmented flows. We used the design of the microfluidic channels to change the flow pattern rather than changing the flow rate of the two streams such that the reaction in a different flow pattern can be compared more directly at the same flow rate.

The schematic diagrams of these devices are shown in Figure 1. Laminar microfluidics flows were created by joining the two streams at a wide T-junction. Preliminary tests had shown laminar flow can be achieved at a wide range of flow rates (tested from 1 to 10 μL/min). Segmented flow microfluidics was created by joining the two streams at a narrow T-junction where the Na_2HPO_4 solution is introduced through a nozzle. The pressure drop through the narrower channel and the nozzle was large enough that the section of wax wall before the nozzle often yields even at low flow rates (e.g., 2 μL/min). A double wall or even triple wall was therefore applied to the section before the nozzle, and the device was found to be stable throughout the experiment. The surfaces of the CaF_2 windows that form the top and bottom parts of the channels were coated with a thin layer of polystyrene to provide a hydrophobic environment for the creation of segmented flow. Polystyrene was used because it has weak spectral bands and it can be cast into thin-film coating with relative ease. The thickness of the polystyrene was estimated from the absorbance of the polystyrene band at 1453 cm^{-1}, and the film thickness was

dx.doi.org/10.1021/ac300019m | *Anal. Chem.* 2012, 84, 4052−4056

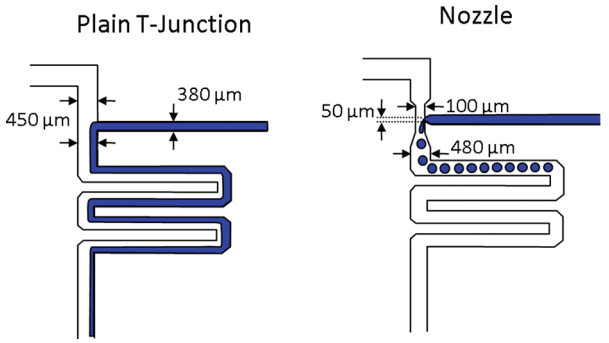

Figure 1. Schematic diagrams showing the design of the microfluidic devices employed in this study. A wider plain T-junction is used to generate a laminar flow profile, whereas a narrow T-junction with a nozzle is used to generate segmented flow profile. The white area inside the channel shows the oil phase which contains benzoic acid while blue area shows the aqueous phase which contains Na_2HPO_4.

found to be 680 nm. Thinner films delaminate easily with fluid flows and therefore are not suitable.

The results for the laminar flow experiment are shown in Figure 2. Benzoic acid and sodium benzoate can be characterized using the spectral bands at 1316 or 1274 cm^{-1} and 1545 or 1383 cm^{-1}, respectively. These bands are selected because they do not overlap with spectral bands of other materials. The integrated absorbances of specific bands are converted into concentrations using calibration curves which can be obtained by measuring the absorbance of solutions with known concentrations using the same spacer of the transmission cell (same path length). The solute concentrations are represented by the color scale of each figure. Figure 2A demonstrates that, away from the interface between the two fluids, the concentration of benzoic acid remains the same, whereas the concentration decreases at the interface. The concentration of sodium benzoate increases from the upstream to the downstream of the channel as the benzoic acid is being neutralized.

Figure 2D is the combined figure of Figure 2A–C such that the three images are overlapped in the form of an RGB map for direct comparisons purpose. Benzoic acid is shown as green, sodium benzoate is shown as red, and water is shown as blue. Figure 2D shows that benzoic acid in decanol (oil phase) did not overlap with water in space while sodium benzoate was formed at the interface between the oil and water and is carried in the aqueous phase rather than the oil phase. Figure 2D also clearly shows the depletion of benzoic acid at the interface downstream which is represented as a dark region between the green region and the red/blue region. This is shown more clearly in the two sets of extracted concentration profiles of benzoic acid and sodium benzoate across the channel width in Figure 3. Data points extracted along lines A and B in Figure 2D, respectively, represent the upstream and downstream concentration profiles of benzoate acid and sodium benzoate. The extracted profiles are an average of five adjacent lines, and the standard deviations between the individual lines are shown as error bars. When the profile extracted along line A to that of line B is compared, it is noted that the concentration of sodium benzoate increased while the concentration of benzoic acid depleted at the interface (starting from left to right), which is consistence with the color figures shown in Figure 2. The depleted region of benzoic acid highlights the lack of mixing across the channel in laminar flow where the rate of the reaction is limited by diffusion. This also demonstrates the power of the presented chemical imaging approach for studies of such flows. The profiles in Figure 3 also show that the concentration decreases near the channel walls. This is due to the scattering effect caused by the difference in refractive index between the wall and the fluids and the roughness of the wax wall resulting in an apparent decrease in concentration.

Better mixing in both oil and aqueous phases is expected in segmented flows.[21] Figure 4 shows the imaging results of the reaction between the two streams in segmented flow. As mentioned previously, the same flow rates that were used in the laminar flow experiment have been applied in the segmented flow experiment. The segmented flow was generated by the design of the microfluidic device. Images were generated based on the specific absorption band of each the component, and the sodium benzoate and benzoic acid data have been calibrated such that the color represents their concentrations. The formation of droplets can be clearly seen immediately after the nozzle in Figure 4A. Since the channel used in this device is relatively wide compared to the size of the droplet, most of the droplets flow along one side of the channel (e.g., more droplets flow along the top side of the section after the first 90° turn and before the first 180° turn). In the first 180° turn, the droplets slowed and start joining together forming slugs which progress further downstream until the end of the microfluidic device. Further refinement of the device such as using narrower channels could have prevented the formation of slugs. However, this is outside the main focus of this work. The image of benzoic acid distribution (Figure 4B) shows that the concentration decreases rapidly after the first 90° turn from 15 wt % to a constant value of approximately 6 wt % after the first

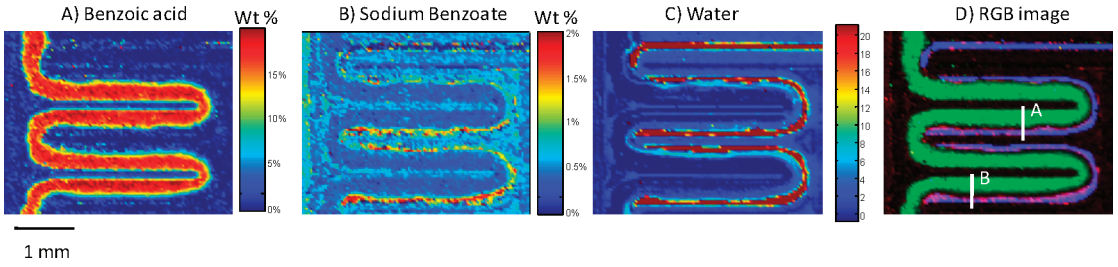

Figure 2. FT-IR imaging results from the device with a wide plain T-junction. (A) FT-IR image showing the concentration (wt %) distribution of benzoic acid in the channel. (B) FT-IR image showing the concentration (wt %) distribution of sodium benzoate in the channel. (C) FT-IR image showing the distribution of water in the channel. Color represents the local concentrations according to the scale shown on the right of the images except the water image which has an arbitrary color scale. (D) An RGB image showing the overlapped images of panels A–C. Benzoic acid is presented in green, sodium benzoate is presented in red, and water is presented in blue.

dx.doi.org/10.1021/ac300019m | *Anal. Chem.* 2012, 84, 4052–4056

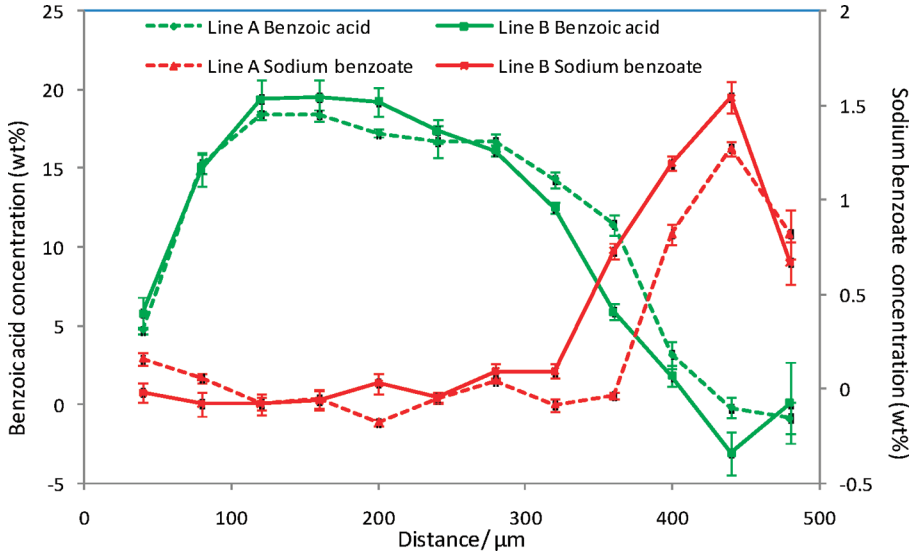

Figure 3. Extracted concentration profiles (average of five adjacent lines) along the lines indicated in Figure 2D.

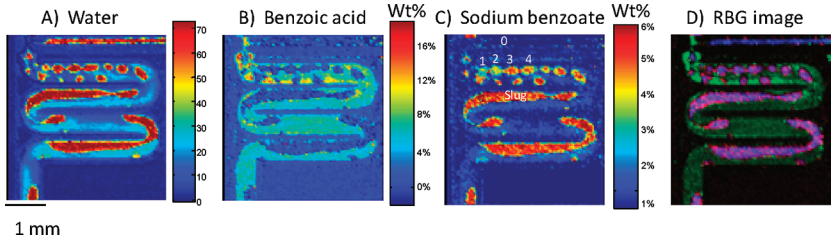

Figure 4. FT-IR imaging results from the device consisting of a narrow T-junction with a nozzle. (A) FT-IR image showing the distribution of water. (B) FT-IR image showing the concentration (wt %) distribution of benzoic acid. (C) FT-IR image showing the concentration (wt %) distribution of sodium benzoate. (D) RGB image showing the overlapped images of panels A–C. Benzoic acid is presented in green, sodium benzoate is presented in red, water is presented in blue.

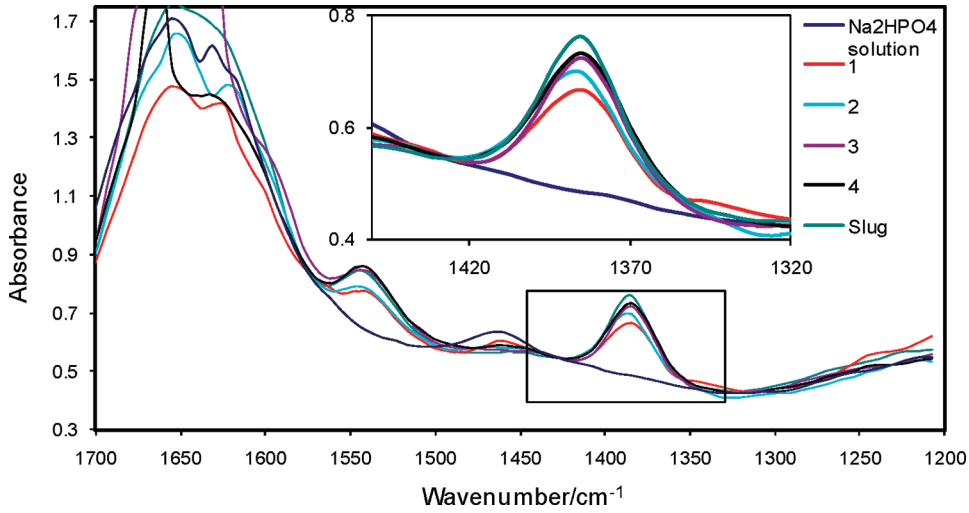

Figure 5. Extracted FT-IR spectra from the indicated points on the image in Figure 4C showing the that concentration of sodium benzoate increases as the Na_2HPO_4 solution droplet progress downstream in the channel.

180° turn. Unlike the laminar flow experiment, where the reaction continues until near the end of the device, the result shows that the concentration of benzoic acid has reached a constant level after the first 180° turn reflecting the fact that the reaction is completed well before the end of the microfluidic device. The reaction did not consume all benzoic acid because benzoic acid was in excess in comparison to Na_2HPO_4.

In the channel after the first 90° turn and before the first 180° turn, the side of the channel with a higher density of Na_2HPO_4 solution droplets has shown a lower benzoic acid concentration than the side that has fewer Na_2HPO_4 droplets. The lack of changes in concentration after the first 180° turn can also be seen in the sodium benzoate image (Figure 4C) which shows a constant concentration of 5–6 wt %. Averaged

dx.doi.org/10.1021/ac300019m | *Anal. Chem.* 2012, 84, 4052–4056

spectra (average of 4−9 pixels, depending on the size of the drop) showing the sodium benzoate band were extracted from different water droplets along the channel indicated in Figure 4C and shown in Figure 5. The extracted spectra did not show significant absorbance of the oil indicating the presented data has minimal spectral contamination from the oil phase, which could be possible when the size of the drop is smaller than the spatial resolution of the system. The absorbance of the sodium benzoate band at 1383 cm^{-1} increases as a function of distance traveled in the channel. Together with the speed of the droplet in the channel, which has been estimated to be 2 mm/s (based on the flow rate of the fluids), one can extract the kinetics of the reaction in the system. Note that the concentration of sodium benzoate already reached ∼50% of the maximum concentration (concentration in the slugs) in the first droplet measured. This result indicates that despite the short amount of contact time with the oil phase, ∼50% of the reaction has happened during the formation of the droplet at the nozzle. An RGB image (Figure 4D) is created to overlap three images for comparison purpose. Sodium benzoate is represented in red, benzoic acid is represented in green, while water is represented in blue. The RGB figure clearly shows that sodium benzoate is carried in the aqueous stream (totally overlapped with the water image). Compared to the RGB image in Figure 2D, there is no depleted region of benzoic acid in the oil phase, which also indicates better mixing is achieved in the segmented flow. This also shows the unique power of the chemical imaging approach applied here to study reactions and mixing in segmented flows in microfluidic devices.

CONCLUSIONS

FT-IR spectroscopic imaging has been shown to be applicable to capture chemical reactions in both laminar flow and segmented flow in microfluidics devices with a two-phase (oil and water) system in a label-free and quantitative manner. Neutralization of benzoate acid in decanol with disodium phosphate in water has been used as the model reaction. The concentrations of both reactant and product can be monitored at any location in the channel of the microfluidic device within the imaged area while concentration profiles can be readily extracted. The reaction rates have been compared between laminar flow microfluidics and segmented flow microfluidics without changing the flow rates of the feed streams. This is achieved by the different design of the microfluidic devices to obtain laminar flow and segmented flow. The reaction is shown to be diffusion-limited in the laminar flow device and the reaction rate is shown to be much higher in segmented flow due to much better mixing. This work demonstrates that FT-IR spectroscopic imaging can be a powerful approach to study reactions in microfluidic devices or microstructured reactors in situ.

ASSOCIATED CONTENT

Supporting Information

Reference spectra of the reactants and products and spectra of the polystyrene film on CaF_2 substrate and the reference standard polystyrene film. This material is available free of charge via the Internet at http://pubs.acs.org.

AUTHOR INFORMATION

Corresponding Author

*E-mail: s.kazarian@imperial.ac.uk.

Notes

The authors declare no competing financial interest.

ACKNOWLEDGMENTS

S.G.K. acknowledges research funding from the European Research Council under the European Community's Seventh Framework Programme (FP7/2007-2013)/ERC advanced grant agreement no. [227950]. We also thank Dr. Xize Niu and Professor Andrew J. deMello for help and advice.

REFERENCES

(1) Jahnisch, K.; Hessel, V.; Lowe, H.; Baerns, M. *Angew. Chem., Int. Ed.* **2004**, *43*, 406−446.
(2) Song, H.; Chen, D. L.; Ismagilov, R. F. *Angew. Chem., Int. Ed.* **2006**, *45*, 7336−7356.
(3) Teh, S. Y.; Lin, R.; Hung, L. H.; Lee, A. P. *Lab Chip* **2008**, *8*, 198−220.
(4) deMello, A. J. *Nature* **2006**, *442*, 394−402.
(5) Aubin, J.; Ferrando, M.; Jiricny, V. *Chem. Eng. Sci.* **2010**, *65*, 2065−2093.
(6) Hill, E. K.; de Mello, A. J. *Analyst* **2000**, *125*, 1033−1036.
(7) Bouchard, L. S.; Burt, S. R.; Anwar, M. S.; Kovtunov, K. V.; Koptyug, I. V.; Pines, A. *Science* **2008**, *319*, 442−445.
(8) Leung, S. A.; Winkle, R. F.; Wootton, R. C. R.; deMello, A. J. *Analyst* **2005**, *130*, 46−51.
(9) Salmon, J. B.; Ajdari, A.; Tabeling, P.; Servant, L.; Talaga, D.; Joanicot, M. *Appl. Phys. Lett.* **2005**, *86*, 094106.
(10) Schafer, D.; Squier, J. A.; van Maarseveen, J.; Bonn, D.; Bonn, M.; Muller, M. *J. Am. Chem. Soc.* **2008**, *130*, 11592−11593.
(11) Liu, G. L.; Lee, L. P. *Appl. Phys. Lett.* **2005**, *87*, 074101.
(12) Xiao, Y.; Yu, X. D.; Wang, K.; Xu, J. J.; Huang, J.; Chen, H. Y. *Talanta* **2007**, *71*, 2048−2055.
(13) Kazarian, S. G. *Anal. Bioanal. Chem.* **2007**, *388*, 529−532.
(14) Chan, K. L. A.; Gulati, S.; Edel, J. B.; de Mello, A. J.; Kazarian, S. G. *Lab Chip* **2009**, *9*, 2909−2913.
(15) Chan, K. L. A.; Niu, X.; deMello, A. J.; Kazarian, S. G. *Anal. Chem.* **2011**, *83*, 3606−3609.
(16) Tan, C. K. C.; Delgass, W. N.; Baertsch, C. D. *Appl. Catal., B* **2009**, *93*, 66−74.
(17) Chan, K. L. A.; Kazarian, S. G. *Vib. Spectrosc.* **2006**, *42*, 130−134.
(18) Waldbaur, A.; Rapp, H.; Lange, K.; Rapp, B. E. *Anal. Methods* **2011**, *3*, 2681−2716.
(19) Chan, K. L. A.; Niu, X. Z.; de Mello, A. J.; Kazarian, S. G. *Lab Chip* **2010**, *10*, 2170−2174.
(20) Rolland, J. P.; Van Dam, R. M.; Schorzman, D. A.; Quake, S. R.; DeSimone, J. M. *J. Am. Chem. Soc.* **2004**, *126*, 2322−2323.
(21) Song, H.; Bringer, M. R.; Tice, J. D.; Gerdts, C. J.; Ismagilov, R. F. *Appl. Phys. Lett.* **2003**, *83*, 4664−4666.